

2019

Water effects on optical canopy sensing for late-season site-specific nitrogen management of maize

Tsz Him Lo

University of Nebraska-Lincoln, tszhimlo@huskers.unl.edu

Daran Rudnick

University of Nebraska - Lincoln, daran.rudnick@unl.edu

Brian Krienke

University of Nebraska - Lincoln, krienke.brian@unl.edu

D. M. Heeren


University of Nebraska-Lincoln, derek.heeren@unl.edu

Yufeng Ge

University of Nebraska - Lincoln, yge2@unl.edu

See next page for additional authors

Follow this and additional works at: <https://digitalcommons.unl.edu/biosysengfacpub>

 Part of the [Bioresource and Agricultural Engineering Commons](#), [Environmental Engineering Commons](#), and the [Other Civil and Environmental Engineering Commons](#)

Lo, Tsz Him; Rudnick, Daran; Krienke, Brian; Heeren, D. M.; Ge, Yufeng; and Shaver, Tim M., "Water effects on optical canopy sensing for late-season site-specific nitrogen management of maize" (2019). *Biological Systems Engineering: Papers and Publications*. 617. <https://digitalcommons.unl.edu/biosysengfacpub/617>

This Article is brought to you for free and open access by the Biological Systems Engineering at DigitalCommons@University of Nebraska - Lincoln. It has been accepted for inclusion in Biological Systems Engineering: Papers and Publications by an authorized administrator of DigitalCommons@University of Nebraska - Lincoln.

Authors

Tsz Him Lo, Daran Rudnick, Brian Krienke, D. M. Heeren, Yufeng Ge, and Tim M. Shaver

Water effects on optical canopy sensing for late-season site-specific nitrogen management of maize

Tsz Him Lo,¹ Daran R. Rudnick,¹ Brian T. Krienke,²
Derek M. Heeren,¹ Yufeng Ge,¹ and Tim M. Shaver³

¹ Department of Biological Systems Engineering, University of Nebraska–Lincoln, USA

² Department of Agronomy and Horticulture, University of Nebraska–Lincoln, USA

³ Wilbur-Ellis Company, USA

Corresponding author — D. R. Rudnick, 402 West State Farm Road,
North Platte, NE 69101, USA; *email* daran.rudnick@unl.edu

Abstract

The interpretation of optical canopy sensor readings for determining optimal rates of late-season site-specific nitrogen application to corn (*Zea mays* L.) can be complicated by spatially variable water sufficiency, which can also affect canopy size and/or pigmentation. In 2017 and 2018, corn following corn and corn following soybeans were subjected to irrigation×nitrogen fertilizer treatments in west central Nebraska, USA, to induce variable water sufficiency and variable nitrogen sufficiency. The vegetation index-sensor combinations investigated were the normalized difference vegetation index (NDVI), the normalized difference red edge index (NDRE), and the reflectance ratio of near infrared minus red edge over near infrared minus red (DATT) using ACS-430 active optical sensors; NDVI using SRSNDVI passive optical sensors; and red brightness and a proprietary index using commercial aerial visible imagery. Among these combinations, NDRE and DATT were found to be the most suitable for assessing nitrogen sufficiency within irrigation levels.

Published in *Computers and Electronics in Agriculture* 162 (2019), pp 154–164.

doi 10.1016/j.compag.2019.04.006

Copyright © 2019 Elsevier B.V. Used by permission.

Submitted 10 January 2019; revised 2 April 2019; accepted 7 April 2019

While DATT was the least sensitive to variable water sufficiency, DATT still tended to decrease with decreasing water sufficiency in high nitrogen treatments, whereas the effect of water sufficiency on DATT was inconsistent in low nitrogen treatments. A new method of quantifying nitrogen sufficiency while accounting for water sufficiency was proposed and generally provided more consistent improvement over the mere averaging of water effects as compared with the canopy chlorophyll content index method. Further elucidation and better handling of water-nitrogen interactions and confounding are expected to become increasingly important as the complexity, automation, and adoption of sensor-based irrigation and nitrogen management increase.

1. Introduction

Adverse market conditions, nitrate contamination of drinking water and aquatic ecosystems, and concerns about fossil fuel depletion and greenhouse gas emissions continue to motivate efforts to reduce nitrogen (N) fertilizer losses in corn (*Zea mays* L.) production. One practice that can contribute to these efforts is late-season N fertilizer application (i.e., during the late vegetative and early reproductive growth stages). This practice can enable growers to adapt to spatiotemporal variability in spring mineralization of organic N and to shorten the time between fertilizer application and late-season plant uptake. A valuable tool for late-season N management is optical canopy sensing. By the late vegetative and early reproductive growth stages of corn, variable N sufficiency generally manifests as deviations in canopy size and/or pigmentation. Optical canopy sensors usually detect these deviations by measuring reflectance at visible and near infrared wavelengths. To infer about N sufficiency, the measurements from the area of interest are typically compared with those from a N sufficient reference area, and a sufficiency index (SI) value is calculated (Blackmer and Schepers, 1995). The advantages of optical canopy sensing include consideration of in-season feedback (unlike simulation models) and efficient sampling of many plants across a large area (unlike chemical analyses of soil or plant tissue).

Yet, N sufficiency may not be the sole factor influencing canopy size and/or pigmentation at a particular growth stage. One of many potential extraneous factors is water sufficiency. At the corn leaf scale, Schepers et al. (1996) and Schlemmer et al. (2005) found that water stress increased reflectance at visible and near infrared wavelengths. At the corn canopy scale, Clay et al. (2006) found that water stress decreased the value of the normalized difference vegetation index (NDVI) during the silking (R1) and blister (R2) growth stages. Shiratsuchi et al. (2011) and Ward (2015) later found that water stress generally decreased the values of multiple reflectance indices that increase with N sufficiency, but this sensitivity to water sufficiency was greater for NDVI than for the Datt (1999) vegetation index. Across a field with significant

soil spatial variability, water sufficiency might be as nonuniform as N sufficiency. There may be spatial differences in hydrological fluxes such as infiltration, deep percolation, and subsurface lateral flow. There may also be spatial differences in the relationship between soil water depletion and water stress severity. If water sufficiency is spatially variable, then its consequent canopy effects can also be spatially variable.

Correctly interpreting optical canopy sensor readings in the presence of variable water sufficiency becomes complicated because deviations in canopy size and/or pigmentation can no longer be simplistically attributed to variable N sufficiency. Comparing an area of interest against a N sufficient reference that was more water sufficient could lead to underestimation of SI and to application of N fertilizer to plants that are water stressed but N sufficient. Conversely, comparing the area of interest against a N sufficient reference that was less water sufficient could lead to overestimation of SI and to withholding of N fertilizer to plants that are N stressed but water sufficient. Because the first type of error can increase N losses while the second type of error can decrease yield, acknowledging the possibility of such error, understanding such error, and developing robust methods to minimize such error are important for the use of optical canopy sensors for late-season site-specific N management.

To narrow this knowledge gap, this research pursued two objectives. The first was to characterize water effects on the values of different combinations of optical sensors and vegetation indices and on their effectiveness in indicating N sufficiency. The second was to evaluate methods for mitigating water effects on N sufficiency determinations.

2. Materials and methods

2.1. Experiment description

The research site was located at the University of Nebraska–Lincoln West Central Research and Extension Center, North Platte, NE, USA. Since 2014, the research site has been under annual summer corn or soybean production without any tillage and any stover removal. All corn was planted at a depth of 0.05m in 0.76m rows parallel to the center pivot wheel tracks and received 47 L ha⁻¹ of ammonium polyphosphate (10–34–0; 6.5 kg ha⁻¹ N) dribbled onto the seed furrow. Irrigation was supplied by groundwater containing 1.5 ppm N (Ward Laboratories, Kearney, NE; 0.4 kg ha⁻¹ N per 25.4mm of irrigation water) through a center pivot with sprayhead sprinklers positioned every other interrow at a height of 0.6m above ground. A GrowSmart Precision Variable Rate Irrigation system (Lindsay Corporation, Omaha, NE) customized the application depth for each plot by changing the end tower speed and

by pulsing a solenoid valve at each outlet. For simplicity, the small amount of N addition ($< 10 \text{ kg ha}^{-1} \text{ N}$ total) by ammonium polyphosphate and irrigation well water was deemed to be negligible in this study. The N fertilizer source for all preplant, sidedress, and fertigation was urea ammonium nitrate (32–0–0). Preplant and sidedress were applied by a double coulter applicator dribbling at a depth of 0.03m and at a distance of 0.19m from the center of the crop row on both sides. Application rate changes between plots were accomplished by a LiquiShift variable rate fertilizer pump (Sure-Fire Ag Systems, Atwood, KS). Fertigation was performed by altering irrigation application depths for each plot as aforementioned while injecting fertilizer at a rate proportional to the irrigation system flow rate. The variable rate injection was governed by a Reflex variable rate fertigation control panel (Agri-Inject, Yuma, CO) that was connected to a McPropeller flow meter (McCrometer, Hemet, CA) and programmed to maintain a constant concentration of 441 ppm N in the irrigation system (corresponding to $112 \text{ kg ha}^{-1} \text{ N}$ applied per 25.4mm of fertigation water).

In 2017 and 2018, two irrigation \times N fertilizer factorial studies were conducted. One study was corn following corn (hereafter CC), and each CC plot remained in the same location and received the same treatment during both years. The other study was corn following soybean (hereafter CS), and each year all CS plots were relocated to a different area that was managed uniformly for irrigated soybean the previous year.

The CC study imposed three irrigation levels \times four N fertilizer levels. The experimental design was strip plot with four replicate blocks. Each experimental unit (i.e., plot) was 11 rows (8.4 m) wide and 36m long. The CC irrigation levels were (1) no irrigation, (2) critical irrigation (i.e., full irrigation only between V14 and R2 and no irrigation otherwise), and (3) full irrigation. The CC N levels were (1) 0 kg ha^{-1} , (2) 67 kg ha^{-1} , (3) 202 kg ha^{-1} , and (4) 269 kg ha^{-1} , with each seasonal N fertilizer rate applied half as preplant and half as sidedress. Hybrid seed corn blend DeKalb 61-54SSRIB (relative maturity rating of 111; Monsanto Company, St. Louis, MO) was planted at $81,500 \text{ seeds ha}^{-1}$. The preplant, emergence, sidedress, silking, and maturity dates were 5 May, 17 May, 12 June, 26 July, and 10 October in 2017 and 19 April, 11 May, 31 May, 14 July, and 14 September in 2018, respectively.

The CS study was two adjacent sub-studies, each imposing a different irrigation level (full versus limited) with four N fertilizer levels while following a randomized complete block design with four replicate blocks. Each plot was 15 rows (11.4 m) wide and 29m long. The N levels of the CS full irrigation sub-study were (1) 0 kg ha^{-1} (i.e., no preplant and no fertigation), (2) limited N (i.e., 34 kg ha^{-1} of preplant and then 34 kg ha^{-1} of weekly fertigation whenever SI for N fell below 0.85 between V8 and R2), (3) full N (i.e., 78 kg ha^{-1} of preplant and then 34 kg ha^{-1} of weekly fertigation whenever SI fell below 0.95 between V8 and R2), and (4) excessive N (i.e., preplant with

supplemental fertigation). The N levels of the CS limited irrigation sub-study were (1) 0 kg ha⁻¹ (i.e., no preplant and no fertigation), (2) limited N (i.e., 56 kg ha⁻¹ in 2017 or 34 kg ha⁻¹ in 2018 of base fertigation around V4 and then 34 kg ha⁻¹ of weekly fertigation whenever SI fell below 0.85 between V8 and R2), (3) full N (i.e., 56 kg ha⁻¹ in 2017 or 34 kg ha⁻¹ in 2018 of base fertigation around V4 and then 34 kg ha⁻¹ of weekly fertigation whenever SI fell below 0.95 between V8 and R2), and (4) excessive N (i.e., fertigation spread between V4 and R2). In 2017, weekly fertigation for the limited N and full N levels was decided for all four plots of a treatment depending on the average SI across those four plots. In 2018, however, weekly fertigation for the limited N and full N levels was decided for each plot individually depending on its SI. Hybrid seed corn blend Fontanelle 6A327RBC (relative maturity rating of 107; Monsanto Company, St. Louis, MO) was planted at 84,000 seeds ha⁻¹ for both CS sub-studies. The preplant, emergence, base fertigation, silking, and maturity dates were 4 May, 16 May, 8 June, 18 July, and 30 September in 2017 and 16 May, 18 May, 1 June, 13 July, and 13 September in 2018, respectively.

2.2. Data collection and processing

The three optical canopy sensors investigated in this research were (1) the Crop Circle ACS-430 (Holland Scientific, Lincoln, NE; Holland Scientific, 2018), a point-based active sensor that emits its own modulated light and measures reflectance at 670 nm (hereafter red), 730 nm (hereafter red edge), and 780 nm (hereafter near infrared); (2) the Spectral Reflectance Sensor (SRS; METER Group, Pullman, WA; METER Group, 2018), a point-based passive sensor that relies on sunlight and measures reflectance at 650 nm (hereafter red) and 810 nm (hereafter near-infrared); and (3) the EOS 5D Mark III (Canon, Tokyo, Japan), a digital camera that assigns a 0–255 brightness value of red, green, and blue to each image pixel. The ACS-430 and the SRS sensors were attached to a tractor-mounted boom (i.e., the sensor platform) at a height of 2.9m above ground. Sensor data was generally collected one or two hours after solar noon on each sensing date. The sensing platform was driven at a speed of 0.6ms⁻¹ in 2017 and 1.3ms⁻¹ in 2018 up and down alleys along the lengthwise edges of the plots so that both the sensors on the left side of the boom and the sensors on the right side of the boom traveled along an inter-row (Shaver et al., 2017) near the middle of each plot exactly once. One ACS-430 on the left side generated ten readings per second in 2017, and two ACS-430 on each of the left and right sides generated five readings per second in 2018. One SRS measuring upwelling radiance on each of the left and right sides and one SRS measuring downwelling irradiance in the middle generated one reading every three seconds in 2017, and no SRS were deployed in 2018. The digital camera was attached to an airplane flying at a

height of 1500m above ground, and one aerial image of the entire field was acquired generally around noon on each sensing date (AirScout, Monee, IL).

Sensor readings from locations where as-applied rates of irrigation and/or N fertilizer were transitioning between different treatment-prescribed rates were filtered and removed. For each plot, readings were excluded if they were outside the middle 4.6m of the plot width or if they were less than 9.1m from each lengthwise end. In 2017, the location of each ACS-430 and SRS reading was determined jointly by a Geo 7X handheld global positioning system (GPS) receiver (Trimble, Sunnyvale, CA) attached to the tractor and by the built-in GPS receiver in the GeoScout X data logger (Holland Scientific, Lincoln, NE) storing the ACS-430 readings. In 2018, the location of each ACS-430 reading was determined by an external differential GPS (DGPS) receiver (Holland Scientific, Lincoln, NE) connected to the GeoScout X data logger. The aerial images had been georeferenced to the World Geodetic System 1984 geographic coordinate system by AirScout, and each pixel generally corresponded to 0.2m×0.2m on the field. For the purpose of this research, the aerial images underwent the adjust transformation in ArcGIS 10.2 (ESRI, Redlands, CA) based on five ground control points surrounding the study areas to further enhance spatial accuracy. The transformed images were then projected to the North American Datum of 1983 Universal Transverse Mercator Zone 14 North projected coordinated system and finally snapped and resampled to the same grid and resolution (0.6 m) as the 2016 National Agricultural Imagery Program image for the county to which this field belonged. This spatial filtering preserved approximately 300 ACS-430 readings and 21 SRS readings per CC plot in 2017, 280 ACS-430 readings per CC plot in 2018, 190 ACS-430 readings and 14 SRS readings per CS plot in 2017, and 175 ACS-430 readings per CS plot in 2018. With the aerial images, this spatial filtering preserved 242 pixels per CC plot and 142 pixels per CS plot in 2017 and 2018.

The readings that passed through the aforementioned filtering were summarized for analysis. For each plot, the median values of red reflectance (ρ_R), red edge reflectance (ρ_{RE}), near infrared reflectance (ρ_{NIR}), normalized difference vegetation index (NDVI; Eq. (1)), red edge normalized difference vegetation index (NDRE; Eq. (2)), and the Datt (1999) reflectance index (DATT; Eq. (3)) from each ACS-430 sensor were calculated, and these median values were averaged across the four ACS-430 sensors in 2018. NDVI and NDRE were default outputs from ACS-430, whereas DATT was identified by past studies to be relatively resistant to water effects (Shiratsuchi et al., 2011; Ward, 2015; Bronson et al., 2017). Likewise, for each plot, the median values of ρ_R , ρ_{NIR} , and NDVI from each downlooking SRS sensor were calculated (Bai et al., 2016), and these median values were averaged across the two upwelling SRS sensors in 2017. With the aerial images, the median values of red brightness (R), green brightness (G), blue brightness (B), and Air-Scout

Difference Vegetation Index (ADVI)—a proprietary index computed from R, G, and B and provided by AirScout—were calculated for each plot. Blackmer and Schepers (1996) found that R decreased with increasing N sufficiency, so R was transformed into R_* (Eq. (4)). Likewise, because ADVI was reported as an integer between 0 and 10,000 by AirScout and seemed to decrease with increasing canopy size and/or greenness, ADVI was transformed into $ADVI_*$ (Eq. (5)).

$$NDVI = \frac{\rho_{NIR} - \rho_R}{\rho_{NIR} + \rho_R} \quad (1)$$

$$NDRE = \frac{\rho_{NIR} - \rho_{RE}}{\rho_{NIR} + \rho_{RE}} \quad (2)$$

$$DATT = \frac{\rho_{NIR} - \rho_{RE}}{\rho_{NIR} - \rho_R} \quad (3)$$

$$R^* = \frac{1 - R}{255} \quad (4)$$

$$ADVI^* = \frac{1 - ADVI}{10000} \quad (5)$$

All datasets used in this research are listed in **Table 1**. Because SRS readings are sensitive to changes in light conditions, SRS datasets that were affected by erratic cloud cover as determined by an SQ-110 hemispherical quantum sensor (Apogee Instruments, Logan, UT) were excluded from all analyses. Aerial images taken during an irrigation or fertigation application were also excluded from all analyses. Additionally, not all datasets were suitable for investigating potential confounding between water sufficiency and N sufficiency in the interpretation of optical canopy sensor readings. An ACS-430 dataset was deemed to be suffering from water effects if NDVI from ACS-430 sensors was numerically lower for the lowest irrigation \times the highest N fertilizer treatment than for the highest irrigation \times highest N fertilizer treatment in all four blocks. In 2017, this criterion was met on six sensing dates between V14 and R4 for the CC study and on six dates between V18 and R4 for the CS study. Rainfall was low from late May to late July in 2017, and later rains could not completely undo the effect of earlier water stress on canopy development. In 2018, the criterion was met by just three dates between V15 and R4 for the CC study and by none of the dates for the CS study. Rainfall was abundant throughout the vegetative and early reproductive growth stages in 2018 except during early July and early August, and the CS limited irrigation level was apparently not severe enough to

Table 1. Optical canopy sensor datasets used in this study; unmarked datasets were included in all analyses, but datasets marked by an asterisk (*) were included only in analyses within irrigation levels because water effects were lacking.

ACS-430	SRS	Aerial Imagery
<i>2017</i>		
17 Jul (CS)	24 Jul (CC & CS)	19 Jul (CC & CS)
19 Jul (CC)	31 Jul (CC)	27 Jul (CC & CS)
24 Jul (CC & CS)	11 Aug (CC & CS)	4 Aug (CC & CS)
31 Jul (CC & CS)	18 Aug (CC & CS)	11 Aug (CC & CS)
11 Aug (CC & CS)	23 Aug (CC)	19 Aug (CC & CS)
18 Aug (CC & CS)		
23 Aug (CC & CS)		
<i>2018</i>		
11 Jul (CC & CS*)		11 Jul (CC & CS*)
19 Jul (CC* & CS*)		9 Aug (CC & CS*)
25 Jul (CC* & CS*)		15 Aug (CC & CS*)
2 Aug (CC & CS*)		
11 Aug (CC & CS*)		

induce noticeable canopy differences before the end of the early reproductive growth stages. The ranges of ACS-430 sensing dates that were deemed to be suffering from water effects were used to select SRS and aerial imagery datasets that were also deemed to be suffering from water effects.

2.3. Data analysis

The six sensor-index combinations were first assessed in terms of reliability to indicate N sufficiency given the same irrigation level. For each irrigation level inside each block, a Kendall's τ rank correlation coefficient (Kendall, 1938) was calculated between the four N fertilizer rates and the corresponding values of a given sensor-index combination. All the correlation coefficients for that sensor-index combination across blocks and irrigation levels were averaged on each day to summarize the strength of that sensor-index combination for indicating N sufficiency when irrigation level was held constant.

Sufficiency index (SI) was calculated by dividing the VI of the plot by the corresponding N sufficient reference value—here taken to be average VI of the treatment with same irrigation level but excessive N (Eq. (6)). The range in SI can differ by sensor-index combination (Holland and Schepers, 2010). Some studies have neglected this possibility and have used the range in SI to conclude about the sensitivity of indices. However, just like changing the display units of a weighing scale does not necessarily increase its precision or accuracy, a larger range in SI does not necessarily imply greater precision

or accuracy of N status assessment. Rather, SI values computed using indices with small SI ranges cannot be directly compared to SI values computed using indices with large SI ranges. On the other hand, the range in SI for a given sensor-index combination may be used to compare study-years in terms of fertilizer responsiveness. SI values were normalized by the range in SI (Eq. (7)) for fairly assessing sensor-index combinations, an integral task of this research. Normalized SI values are compatible with linear relationships between SI values using different indices (Solari et al., 2008) and with quadratic models of SI response to N fertilizer (Holland and Schepers, 2010). Impact of neglecting variable water sufficiency was simulated by substituting the N sufficient reference and the nonfertilized check of the same irrigation level with the full irrigation \times excessive N and the full irrigation \times 0 kg ha⁻¹ N treatments, respectively (Eqs. (8)–(9)).

$$SI = \frac{VI}{VI_{i\text{ref},l}} \quad (6)$$

$$SI_i^* = \frac{SI_i - SI_{0,i}}{1 - SI_{0,i}} = \frac{VI - VI_{0,i}}{VI_{\text{ref},i} - VI_{0,i}} \quad (7)$$

$$SI_{ws} = \frac{VI}{VI_{\text{ref},ws}} \quad (8)$$

$$SI_{ws}^* = \frac{SI_{ws} - SI_{0,ws}}{1 - SI_{0,ws}} = \frac{VI - VI_{0,ws}}{VI_{\text{ref},ws} - VI_{0,ws}} \quad (9)$$

where

SI_i = sufficiency index with perfect knowledge of irrigation level

VI = vegetation index for the plot of interest

$VI_{\text{ref},i}$ = average vegetation index for the excessive N level given the same irrigation level as the plot of interest

SI_i^* = normalized sufficiency index with perfect knowledge of irrigation level

$SI_{0,i}$ = sufficiency index for the nonfertilized level given the same irrigation level as the plot of interest

$VI_{0,i}$ = average vegetation index for the nonfertilized level given the same irrigation level as the plot of interest

SI_{ws} = sufficiency index with water sufficient assumption

$VI_{\text{ref},ws}$ = average vegetation index for the full irrigation \times excessive N treatment

SI_{ws}^* = normalized sufficiency index with water sufficient assumption
 $SI_{0,ws}$ = sufficiency index for the full irrigation×nonfertilized treatment
 $VI_{0,ws}$ = average vegetation index for the full irrigation×nonfertilized treatment

Moran et al. (1994) introduced a two-dimensional method of calculating crop water stress index (Idso et al., 1981; Jackson et al., 1981) that aims to account for partial canopy cover by introducing the soil adjusted vegetation index (Huete, 1988) as an indicator of canopy cover. Likewise, two-dimensional methods of calculating normalized SI aim to account for a non-N factor by introducing a second variable as an indicator of that non-N factor. Attempting to obtain normalized SI values that solely represent N sufficiency without the confounding of season-to-date water sufficiency, this research proposed a new two-dimensional method (**Fig. 1**) of calculating normalized SI based on the trapezoid concept of Moran et al. (1994). The second variable for this new method is normalized canopy temperature (T_c^* ; Eq. (10)), measured at a time when spatial variability in canopy temperature is large and reveals the typical pattern of season-to-date water sufficiency across the field. In this research, canopy temperature was measured in the midafternoon of 24 July 2017 for CC 2017 and CS 2017 and in the midafternoon of 11 August 2018 for CC 2018 by SI-1H1 infrared thermometers (Apogee Instruments, Logan, UT) attached to the same tractor-mounted boom as the optical canopy sensors. Assuming season-to-date water sufficiency is unknown *a priori*, the new method first determined the linear regression relationship between DATT and T_c^* for excessively N fertilized plots and for nonfertilized plots, respectively. The two regression relationships were then used to interpolate the DATT values of the N sufficient reference and the nonfertilized check that correspond to T_c^* of any area of interest. Finally, normalized SI for the area of interest is calculated using the interpolated DATT values of the N sufficient reference and the nonfertilized check (Eq. (11)).

$$T_c^* = \frac{T_c - T_{c,min}}{T_{c,max} - T_{c,min}} \quad (10)$$

$$SI_t^* = \frac{DATT - (a_0 T_c^* + b_0)}{(a_1 T_c^* + b_1) - (a_0 T_c + b_0)} \quad (11)$$

where

T_c^* = normalized canopy temperature for the plot of interest
 T_c = canopy temperature for the plot of interest measured at a time when spatial variability in canopy temperature is large and

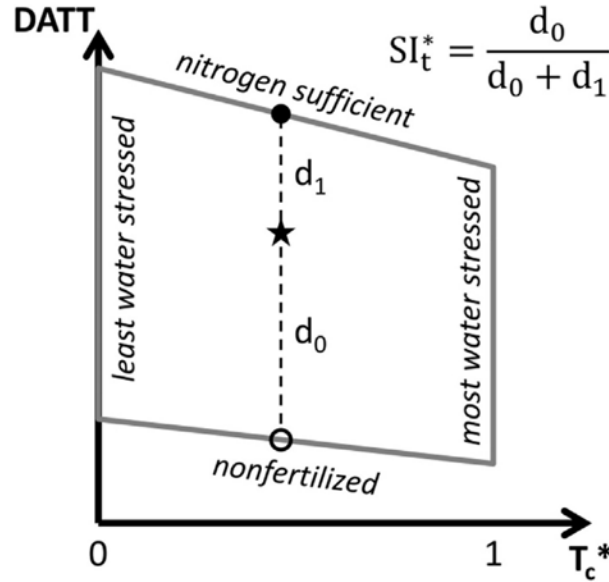


Fig. 1. Theoretical illustration of the new method of calculating normalized sufficiency index while accounting for water effects.

reveals the typical pattern of season-to-date water sufficiency across the field

$T_{c,min}$ = canopy temperature of the coldest plot in the field, measured at (nearly) the same time as T_c

$T_{c,max}$ = canopy temperature of the hottest plot in the field, measured at (nearly) the same time as T_c

SI_t^* = normalized sufficiency index whose N sufficient reference and nonfertilized check are interpolated using regression between DATT and T_c^* based on excessively fertilized and nonfertilized areas with a wide range in season-to-date water sufficiency

DATT = value of the Datt (1999) index for the plot of interest

a_0 = slope of the DATT versus T_c^* line based on nonfertilized areas with a wide range in season-to-date water sufficiency

b_0 = intercept of the DATT versus T_c^* line based on nonfertilized areas with a wide range in season-to-date water sufficiency

a_1 = slope of the DATT versus T_c^* line based on excessively fertilized areas with a wide range in season-to-date water sufficiency

b_1 = intercept of the DATT versus T_c^* line based on excessively fertilized areas with a wide range in season-to-date water sufficiency

Another two-dimensional method of calculating normalized SI is the canopy chlorophyll content index (CCCI), which was originally proposed by

Barnes et al. (2000) to account for partial canopy cover. Past studies had used CCCI to assess N sufficiency in wheat and cotton under variable water sufficiency (Fitzgerald et al., 2006; Tiling et al., 2007; El-Shikha et al., 2008). Again assuming water sufficiency is unknown *a priori*, CCCI first determined the linear regression relationship between NDRE and NDVI for excessively fertilized areas and for nonfertilized areas, respectively. The intercepts of both lines were held at zero. These regression relationships were then used to interpolate the NDRE values of the N sufficient reference and the nonfertilized check that correspond to the NDVI value of any area of interest (Eq. (12)).

$$CCCI = \frac{NDRE - (c_0 NDVI)}{(c_1 NDVI) - (c_0 NDVI)} \quad (12)$$

where

CCCI = canopy chlorophyll content index for the plot of interest

NDRE = normalized difference red edge index for the plot of interest

NDVI = normalized difference vegetation index for the plot of interest

c_0 = slope of the NDRE versus NDVI line based on nonfertilized areas with a wide range in water sufficiency

c_1 = slope of the NDRE versus NDVI line based on excessively fertilized areas with a wide range in water sufficiency

3. Results and discussion

3.1. Comparisons within irrigation levels

Sensor-index combinations differed in their effectiveness in indicating N sufficiency under the same irrigation level for late-season N management. With the ACS-430 sensor, NDRE and DATT were consistently more effective than NDVI. NDRE and DATT exhibited relatively high average τ , signifying strong correlation with N fertilizer rate at the same irrigation level within each block (**Fig. 2a**). These two indices also exhibited relatively low average standard deviation (SD) in normalized SI (SI_i^* ; Eq. (7)), signifying small variability in SI_i^* among replicates of each irrigation \times N fertilizer treatment (Fig. 2c). Therefore, in agreement with Shiratsuchi et al. (2011) and Shaver et al. (2017), NDRE and DATT would be recommended over NDVI for use with ACS-430 sensors for assessing N sufficiency under the same irrigation level for late-season N management.

With aerial visual imagery, R_v was similar in effectiveness to ADV_i^* in all study-years, and both indices tended to exhibit average τ values comparable with ACS-430 NDRE and DATT (Fig. 2a). This result is positive because

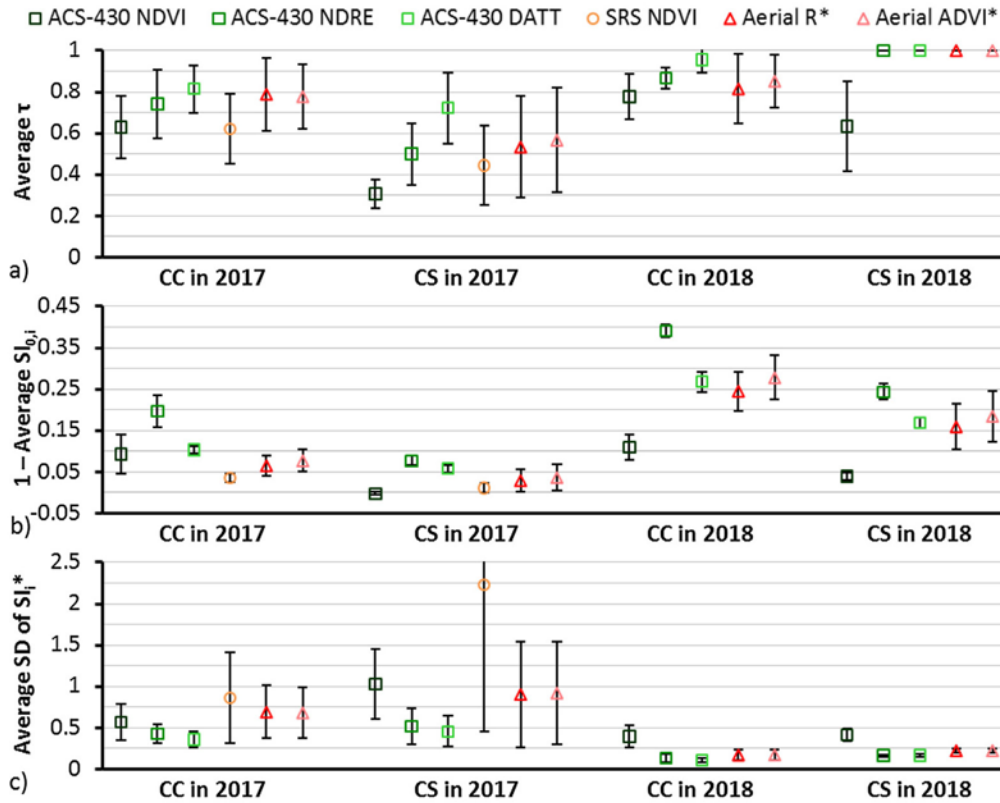


Fig. 2. Study-year averages of (a) Kendall's τ rank correlation coefficient between nitrogen fertilizer rate and sensor-index combination at the same irrigation level within each block, (b) sufficiency index (SI) range expressed as 1 – average SI of the nonfertilized check ($SI_{0,i}$) at each irrigation level, and (c) standard deviation (SD) of normalized SI (SI_i^*) among replicates of each irrigation \times nitrogen fertilizer treatment; error bars denote standard deviation among sensing dates.

aerial visual imagery is generally easier to obtain than ACS-430 measurements. However, average SD of SI_i^* tended to be larger for R_* and $ADVI_*$ than for ACS-430 NDRE and DATT, which suggests that N sufficiency assessment would be noisier using R_* and $ADVI_*$ than using ACS-430 NDRE and DATT (Fig. 2c). Average SD of SI_i^* for R_* and $ADVI_*$ reached almost 1 in CS 2017, meaning that the within-treatment variability in VI was often of similar magnitude to the range in VI between the excessive N and nonfertilized levels at the same irrigation level. Scharf and Lory (2002) found at mid vegetative growth stages that N sufficiency assessment from imagery became less noisy when solely examining pure leaf pixels after filtering out mixed pixels. Although canopy cover is typically full during the late vegetative and early reproductive growth stages, pixels that are at least partially composed of soil, tassels, and shadows would not be the best indicators of N sufficiency. Perhaps even late-season N sufficiency assessment using aerial visible imagery

would benefit from choosing an extremely high image resolution and filtering out such mixed pixels. The original image resolution (0.2 m) was not high enough to enable these pixels to be filtered out, so the R_s and $ADVI_s$ results presented in this research were not artifacts of subsequent resampling to a coarser resolution.

Overall, SRS NDVI was the least effective sensor-index combination among the six investigated in this research. In general, the SRS NDVI exhibited low average τ (Fig. 2a) and large average SD of SI_i^* (Fig. 2c). SRS NDVI might have been encountering the saturation issue that is commonly observed in passive sensor data. The red and near infrared reflectance values reported by SRS both tended to be lower than those reported by ACS-430, and the resultant NDVI values tended to be higher from SRS than from ACS-430. Also, the measurement speed of the SRS sensor relative to the travel speed of the tractor platform was perhaps problematic. The longer measurement time (0.6 s versus 0.1 s) and larger field of view (36° versus $30^\circ \times 15^\circ$) of SRS sensors (METER Group, 2018) versus ACS-430 sensors (Holland Scientific, 2018) may have reduced the sensitivity of SRS sensors to canopy size and/or pigmentation in on-the-go sensing.

As mentioned earlier, the range in SI can vary substantially among sensor-index combinations, with ACS-430 NDRE consistently exhibiting the largest range in all study-years. For example, $1 - \text{average } SI_{0,i}$ of the nonfertilized check ($SI_{0,i}$) was about six times larger for ACS-430 NDRE than for SRS NDVI in CC 2017 and for ACS-430 NDVI in CS 2018 (Fig. 2b). While a large $1 - \text{average } SI_{0,i}$ alone does not imply that ACS-430 NDRE is effective at distinguishing between N levels, this observation reiterates the inappropriateness of direct comparisons between SI values calculated from different sensor-index combinations. Prior normalization (Eq. (7)) or custom calibrations (Solari et al., 2008) would be generally necessary.

Fig. 2 illustrated differences not only among sensor-index combinations but also among study-years. Ranked in ascending order of fertilizer responsiveness as indicated by $1 - \text{average } SI_{0,i}$, the study-years were CS 2017, CC 2017, CS 2018, and CC 2018 (Fig. 2b). The difference in responsiveness between cropping systems is expected at least partly because N mineralization tends to be higher following soybean than corn, which is often called the soybean N credit (Shapiro et al., 2008). Weather differences between the two years also resulted in higher N mineralization in 2017 than 2018. Spring 2017 was relatively warm, and in general, only the nonfertilized check was visually distinguishable from the other N levels. Spring 2018 was relatively cool, and crop appearance of the various N levels diverged remarkably and as early as the mid vegetative growth stages. In short, the larger indigenous N supply in CS than in CC and in 2017 than in 2018 caused a narrower spread in N sufficiency among N levels. For CS 2017, the spread was so small that even nonfertilized checks tended to have $SI_{0,i}$ of at least 0.9 for

all sensor-index combinations investigated, which is close to the common SI threshold of 0.95 for in-season N application (Blackmer and Schepers, 1995). In contrast, treatment induced differences in residual N from the previous year may have further widened the spread in N sufficiency among N levels for CC 2018. Higher N responsiveness of a study-year was associated with higher average τ (Fig. 2a) and with smaller average SD of SI_i^* (Fig. 2c) across sensor-index combinations. The increasing dominance of N fertilizer rate as a determining factor of canopy size and/or pigmentation diminished the relative influence of spatial variability in indigenous N supply and in non-N factors.

3.2. Comparisons across irrigation levels

Water effects were different on the N sufficient reference versus the nonfertilized check for all sensor-index combinations investigated. The VI value of the N sufficient reference generally increased with increasing irrigation level (Fig. 3). Where N was abundant, the crop took advantage of greater water sufficiency to improve the growth and maintenance of its canopy. In contrast, the VI value of the nonfertilized check was usually highest at the critical irrigation level in CC 2017 and CC 2018 (Fig. 3). Where N was limiting, crop water use may be reduced (Rudnick and Irmak, 2014). Thus, the full irrigation

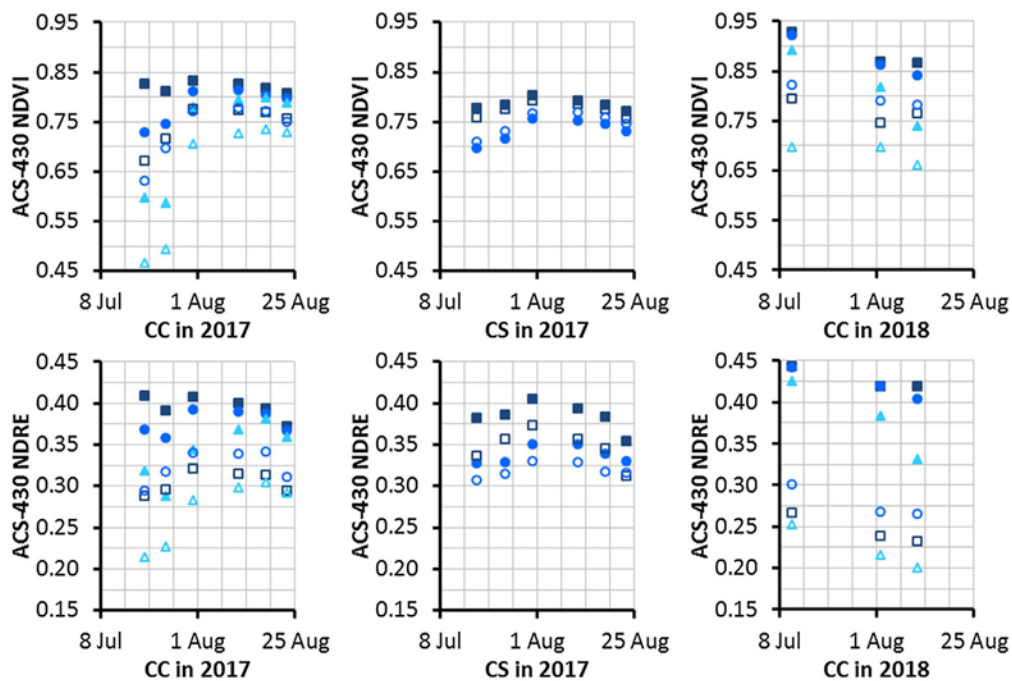


Fig. 3. Treatment average vegetation index values of the nitrogen sufficient reference and the nonfertilized check for various irrigation levels during three study-years.

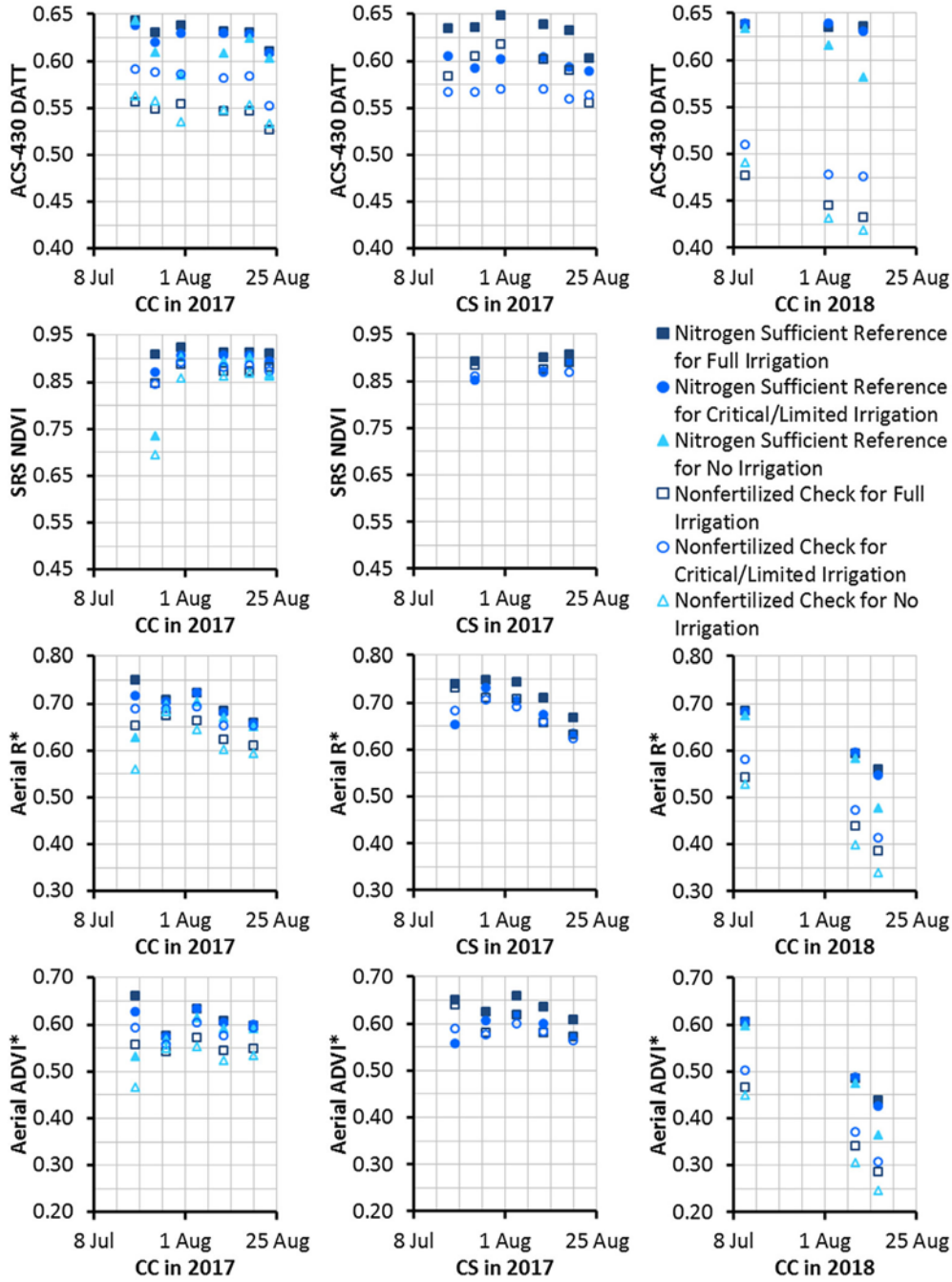


Fig. 3. (continued)

level may be supplying excessive water and ultimately decreasing crop yield (Rudnick et al., 2016), whereas the critical irrigation level was more appropriate for the low N condition. Yet, unlike the critical irrigation level in CC 2017, the limited irrigation level in CS 2017 witnessed much lower VI values

in both its N sufficient reference and its nonfertilized check as compared with the full irrigation level (Fig. 3). Consequently, the VI separation between the two irrigation levels of CS 2017 was large for the N sufficient reference, and the VI value of the nonfertilized check in CS 2017 was generally highest for full irrigation rather than limited irrigation. Because the timing and seasonal amount (102mm versus 122 mm) of irrigation were similar between critical irrigation in CC 2017 and limited irrigation in CS 2017, the disparity in water effects was unexpected. Whether this disparity in water effects was caused by differences in genetics and/or previous crop is unclear. On the other hand, the no irrigation level was fairly consistent in displaying the lowest VI values among irrigation levels in CC 2017 and CC 2018 for both the N sufficient reference and the nonfertilized check (Fig. 3), which was expected.

Intraseasonal trends in VI separation between irrigation levels were also different among study-years. With aerial imagery, the separation tended to be at its minimum during pollination in both CC 2017 and CS 2017 (Fig. 3). Visual inspection of this aerial image revealed that the study area as a whole appeared lighter and yellower on 27 July 2017 than on the immediately previous and following image dates. The influence of corn tassels on aerial and satellite images is widely known, and the interrow positioning of the tractor-mounted ACS-430 and SRS sensors most likely explained why these two sensors were not affected in a similar manner. In contrast, the separation among irrigation levels in CC 2017 was sharply reduced for ACS-430 NDVI, ACS-430 NDRE, and SRS NDVI between 24 and 31 July (Fig. 3). The critical irrigation and no irrigation levels of CC 2017 increased in VI rapidly in response to a large rainfall between 28 and 29 July at the end of a long dry period. Yet in CS 2017, the narrowing of the separation between irrigation levels after this rain event may have occurred to a small extent for ACS-430 NDVI but was not observed for ACS-430 NDRE and SRS NDVI (Fig. 3). This disparity between the limited irrigation level of CS 2017 and the critical irrigation and no irrigation levels of CC 2017 may have been caused by differences in genetics and/or development (CC 2017 was approximately one week behind CS 2017 at this time). At the cessation of water stress, the critical irrigation and no irrigation levels of CC 2017 may have been somehow more capable of undergoing beneficial changes in leaf physiology (e.g., pigment production, chloroplast movement) and morphology (e.g., unrolling) and/or of compensatory canopy expansion enabled by possible delayed entry into the reproductive growth stages. Afterwards, the magnitude of separation among irrigation levels in CC 2017 and CS 2017 each persisted for the rest of the sensing period (Fig. 3), when temperatures were relatively cool and rain was generally plentiful. On the other hand, the CC 2018 sensing period corresponded to a drying trend, and the consequent increasing severity of water stress caused increasing separation among irrigation levels for all sensor-index combinations investigated (Fig. 3).

Because water effects impacted all sensor-index combinations investigated, errors would occur from incorrectly assuming all plots to be water sufficient and thus always using the N sufficient reference and the nonfertilized check of the full irrigation level in the calculation of normalized sufficiency index (SI_* ; i.e., applying Eq. (9) instead of Eq. (7)). With ACS-430 NDVI and NDRE, the mean bias in SI_* tended to be increasingly negative with increasing water stress in all study-years (**Fig. 4**), owing to wider VI separation between irrigation levels (Fig. 3). This phenomenon explains not only intraseasonal trends but also the differences between the critical irrigation and no irrigation subfigures and between the CC 2017 and CC 2018 subfigures (Fig. 4). In contrast, the mean bias in SI_* for SRS NDVI was quite unpredictable. For example, both extremely positive and extremely negative mean biases in SI_*

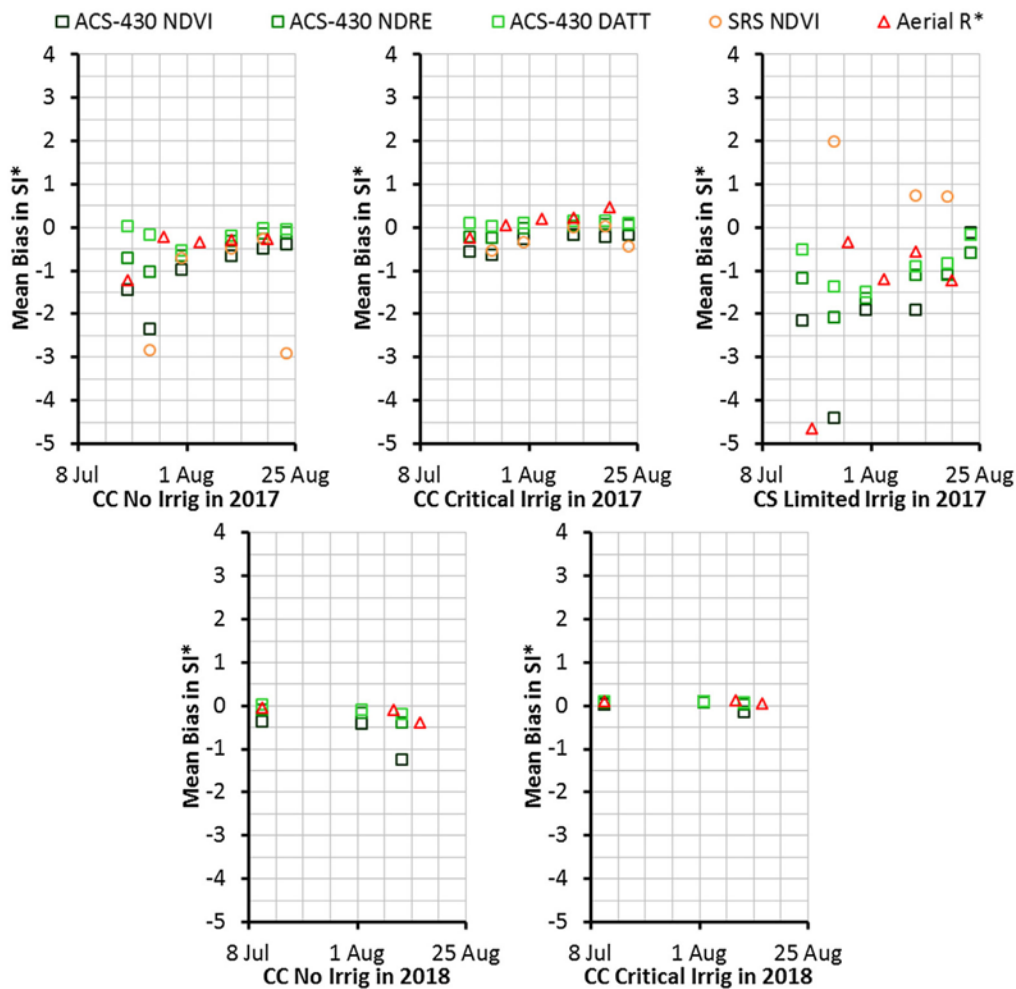


Fig. 4. Mean bias in normalized sufficiency index (SI_*) at different irrigation levels for various sensor-index combinations if all plots were assumed to be sufficient in water; $ADVI^*$ data was not shown because it was nearly identical to R^* data.

were observed for SRS NDVI at the limited irrigation level of CS 2017 (Fig. 4). Such extremes occurred on the first two SRS NDVI sensing dates in CS 2017, when SRS NDVI was actually slightly higher in the nonfertilized check than in the N sufficient reference for the limited irrigation level (Fig. 3). These narrow and inverted VI ranges, which caused extreme instability in SI_x calculations, were the products of applying a poor indicator of N sufficiency during a study-year with small N response (Fig. 2). R_x and $ADVI_x$ were also higher in the nonfertilized check than in the N sufficient reference for the limited irrigation level during the first aerial image date in CS 2017 (Fig. 3), which resulted in a large negative mean bias (Fig. 4). While N response was small in CS 2017, water response and mean bias in SI_x were large. With all sensor-index combinations investigated, the N sufficient reference for limited irrigation was lower in VI than the nonfertilized check for full irrigation on at least one sensing date in CS 2017 (Fig. 3). In these instances, the SI of the N sufficient reference for limited irrigation should be 1, but became a negative value with the water sufficient assumption (Fig. 4), which would be a large error. On the other hand, smaller errors would result when the VI range between the N sufficient reference and the nonfertilized check for full irrigation were mostly overlapping the corresponding range for lower irrigation levels. Readers should note that mean bias in SI_x does not present a full picture of SI_x errors with the water sufficient assumption. In instances when the VI range between the N sufficient reference and the nonfertilized check for a lower irrigation level fell entirely within the corresponding range for full irrigation (or vice versa), both positive biases and negative biases would result. In fact, this situation was common for the critical irrigation level in both CC 2017 and CC 2018 (Fig. 3). Practitioners should be aware of the potential co-occurrence of the positive and negative biases with the water sufficient assumption because site-specific optical canopy sensing for late-season N management aims to achieve accuracy at the subfield scale and not merely zero mean bias at the field scale.

Among the sensor-index combinations investigated, ACS-430 DATT was generally the least sensitive to water effects. In CC 2017, the N sufficient reference and the nonfertilized check for no irrigation were surprisingly similar in ACS-430 DATT to those for full irrigation (Fig. 3), which resulted in relatively small mean bias in SI_x (Fig. 4). The advantages of ACS-430 DATT were also observed on some sensing dates for other irrigation levels and in other study-years (Fig. 4). While ACS-430 DATT was once again found to be more resistant to water effects than were other common VIs (Shiratsuchi et al., 2011; Ward, 2015; Bronson et al., 2017), ACS-430 DATT is certainly not immune to water effects. The mean bias in SI_x with ACS-430 DATT was worse than -0.5 on multiple sensing dates across multiple study-years (Fig. 4), so it is desirable to improve the distinction of water stress and N stress in optical canopy sensing beyond merely using ACS-430 DATT.

So far in this research, the VIs of plots were compared against the treatment average VI of the no N fertilizer level and the excessive N fertilizer level at a particular irrigation level. One might wonder whether water effects would be removed if a virtual reference was used instead. This statistical approach relies on the VI at a chosen percentile of the data as the N sufficient reference instead of imposing and sensing an excessively fertilized area (Holland and Schepers, 2013). Holland and Schepers (2013) noted that the VI value at a chosen percentile was generally higher whenever the canopy condition was better. This same trend was observed in the data of this research, with the VI value at a chosen percentile inside a plot being systematically altered by both variable water sufficiency and variable N sufficiency. Holland and Schepers (2013) recommended practitioners to avoid starting sensing in the most N deficient parts of the field and also to expand continually the dataset from which the VI value at a chosen percentile would be calculated. However, because this original protocol ignores spatial variability of all non-N properties including water, it would not be ideal for fields where the spatial distribution of water sufficiency was unknown. Where to keep or recalculate the virtual reference would be unclear even though water sufficiency can change the N sufficient (and the nonfertilized) values of all sensor-index combinations investigated (Fig. 3). The virtual reference approach may be applied within known areas of similar water sufficiency, but the data of this research would suggest that following the original protocol of this approach would not automatically account for variable water sufficiency.

3.3. Two-dimensional methods

Previous researchers have proposed the inclusion of soil moisture and/or canopy temperature data to help isolate variable N sufficiency from optical canopy sensing data in the presence of variable water sufficiency. Theoretically, the most accurate approach of quantifying variable season-to-date water sufficiency may be to calculate for every part of the field either cumulative actual ET (ET_a) or cumulative daily ratio of ET_a over water sufficient ET. Infrequent soil moisture and/or canopy temperature measurements would be unsuitable for this approach unless the soil and plant characteristics throughout the field were understood adequately for using mathematical models to simulate the conditions between each measurement date. Instead, spatiotemporally dense soil moisture and/or canopy temperature measurements would be needed starting no later than the mid vegetative growth stages because any water stress occurring up to the time of optical canopy sensing can affect canopy size and/or pigmentation. The current cost of acquiring such data, however, would be prohibitive especially

for commercial crop production. Making soil moisture and/ or canopy temperature measurement simultaneously with optical canopy sensing and then inferring season-to-date water sufficiency from this one-time dataset might seem to be an attractive alternative. Nevertheless, whether a unique relationship exists between current water sufficiency and season-to-date water sufficiency would depend on the time of measurement and the season-to-date weather conditions. Trying to schedule optical canopy sensing around the existence of this unique relationship may not be ideal.

An approach that is likely to be both reliable and feasible would be the delineation of water sufficiency zones. Although season-to-date water sufficiency is constantly changing, its spatial pattern is often temporally stable (Vachaud et al., 1985; Barker et al., 2017). Spatial data on crop (e.g., yield maps, thermal imagery) and soil (e.g., apparent electrical conductivity surveys, digital elevation models) continues to become increasingly available. Practitioners can use their understanding of a field to select the data layer(s) that would best describe the spatial pattern of season-to-date water sufficiency. Making soil moisture and/or canopy temperature measurements continuously or simultaneously with optical canopy sensing is unnecessary for the zonal approach because it does not rely on actually knowing instantaneous or season-to-date water sufficiency. For the zonal approach, the best thermal images would be those with maximum contrast—acquired in hot, sunny, dry, and windy midafternoons during periods when water stress of varying severity is prevalent throughout much of the field. Once season-to-date water sufficiency zones have been successfully delineated, zone-specific N sufficient references and nonfertilized checks can be established for assessing N sufficiency within each zone— just like SI_i^* (Eq. (7)) in this research. In the short term, the zonal approach may be the most promising method of accounting for water effects in optical canopy sensing and should be ready to be evaluated on fields with real (i.e., not experimentally imposed) spatial variability.

While the zonal approach is elegant, there may be fields where the spatial pattern of season-to-date water sufficiency cannot be delineated neatly into zones. If season-to-date water sufficiency relative to the rest of the field can be represented by a proxy variable, practitioners could establish N sufficient references and nonfertilized checks across a wide range in the proxy variable. Then, the N sufficient and nonfertilized VI values for each area of interest could be estimated based on the value of the proxy variable in that area of interest. A method that uses this particular approach to calculate normalized SI is hereafter referred to as a two-dimensional method because it involves both an optical canopy sensor VI and a proxy variable indicating season-to-date water sufficiency relative to the rest of the field.

Three practical methods for handling water effects were compared in terms of how closely the resultant normalized SI values matched those

calculated from DATT with perfect knowledge of irrigation level (i.e., SI_i^*). The first method was not a two-dimensional method. It used DATT and merely averaged water effects by pooling all excessively fertilized plots (regardless of irrigation level) as the N sufficient reference and all nonfertilized plots (regardless of irrigation level) as the nonfertilized check. The second method was a newly proposed two-dimensional method (Figs. 1 & 5), which used DATT as the VI and normalized canopy temperature (T_c^*) as the proxy variable (Eqs. (10)–(11)). The third method is the two-dimensional method of canopy chlorophyll content index (Barnes et al., 2000), which used NDRE as the VI and NDVI as the proxy variable (Eq. (12)).

The first method was inherently unable to remove water effects, but the method did center at zero the differences between its normalized SI values (SI_{avg}^*). Thus, the mean difference of SI_{avg}^* from SI_i^* was quite consistently the smallest among the three methods. The root mean square difference (RMSD) of SI_{avg}^* from SI_i^* , however, were large on exactly the same dates when the water sufficient assumption caused large mean biases in SI_i based on DATT (Fig. 4; Table 2). The second method was generally most capable

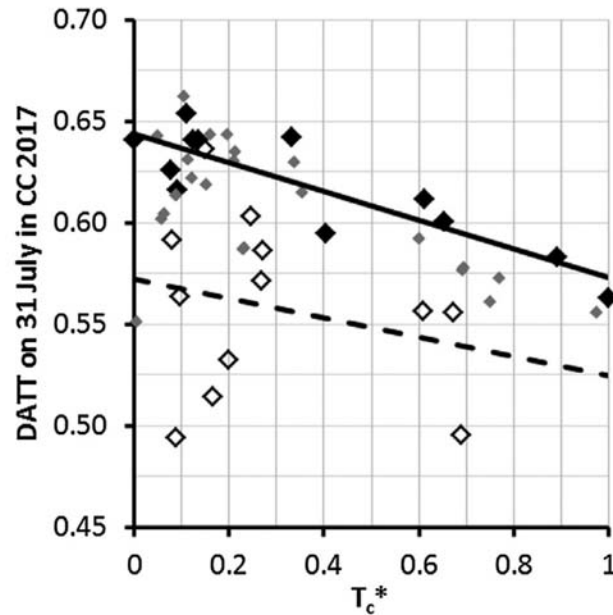


Fig. 5. The Datt (1999) vegetation index (DATT) on 31 July plotted against normalized canopy temperature (T_c^*) in the hot, sunny, dry, and windy midafternoon of 24 July for CC 2017—serving as a realistic counterpart to Fig. 1 for depicting the new method of calculating normalized sufficiency index while accounting for water effects; the nitrogen sufficient reference was represented by large solid diamonds and the solid line, the nonfertilized check was represented by large hollow diamonds and the dashed line, and all other plots were represented by small grey diamonds.

Table 2. Root mean square difference between normalized sufficiency index values calculated using three methods of handling water effects in optical canopy sensing, as compared with normalized sufficiency index values calculated from DATT with perfect knowledge of irrigation level.

CC 2017				CS 2017				CC 2018			
Date	SI_{avg}^*	SI_t^*	CCCI	Date	SI_{avg}^*	SI_t^*	CCCI	Date	SI_{avg}^*	SI_t^*	CCCI
19 Jul	0.13	0.13	0.41	17 Jul	0.29	0.28	0.23	11 Jul	0.06	0.06	0.08
24 Jul	0.25	0.24	0.47	24 Jul	0.76	8.37	0.59	2 Aug	0.08	0.07	0.08
31 Jul	0.40	0.28	0.41	31 Jul	0.75	0.50	0.64	11 Aug	0.14	0.12	0.13
11 Aug	0.21	0.17	0.21	11 Aug	0.47	0.33	0.38				
18 Aug	0.16	0.15	0.19	18 Aug	0.47	0.31	0.42				
23 Aug	0.11	0.11	0.15	23 Aug	0.23	0.32	0.27				

of removing water effects. The RMSD of its normalized SI values (SI_t^*) from SI_i^* was smaller than that of SI_{avg}^* on five out of six dates in CC 2017, four out of six dates in CS 2017, and two out of three dates in CC 2018 (table 2). The second method performed reasonably even when the relationship between DATT and T_c was weak among N sufficient and/or nonfertilized plots. In these cases, the second method essentially averaged the DATT value among N sufficient and/or nonfertilized plots just as the first method would. The second method, however, performed poorly on 24 July in CS 2017 (Table 2). On this date, a substantial proportion of N sufficient plots and nonfertilized plots were indistinguishable from each other in terms of both DATT and T_c^* . The two resultant DATT vs T_c^* regression lines representing the N sufficient reference and the nonfertilized check, respectively, intersected at a T_c^* value between 0 and 1, causing some plots to be compared against small and inverted SI ranges and thus to be assigned extremely erroneous SI_t^* values. The same problem was identified earlier in the research as a frequent cause of large mean biases in SI_i with the water sufficient assumption (Fig. 4). Future research on and application of the second method should include procedures and mechanisms to check for and deal with problematic scenarios. As for the third method, the RMSD of its normalized sufficiency index (CCCI) from SI_i^* was smaller than that of SI_{avg}^* on zero dates in CC 2017, five dates in CS 2017, and two dates in CC 2018.

Admittedly, the overall improvement achieved by the second method was small in this research. Nonetheless, this initial proof-of-concept demonstrated that water effects on optical canopy sensing are not an insurmountable problem and could be intentionally reduced using practical, science-based methods. Colleagues are invited to advance the second method and to test it under diverse circumstances. Given the non-monotonic response of VIs to increasing water sufficiency in the nonfertilized check under some circumstances (Fig. 3), nonlinear regression relationships between DATT and

T_c^* for the nonfertilized check could be explored. Also, future studies could experiment with the use of proxy variables other than T_c^* .

Interestingly, a negative association between canopy temperature and N fertilizer rates appeared to be larger and stronger at higher irrigation levels in CC 2018. This trend was also observed by Tiling et al. (2007) and Mon et al. (2016), and it was unlikely to be coincidental that CC 2018 was the study-year with the largest N response. Canopy temperature can be elevated by N stress via reductions in canopy size and in stomatal conductance (Radin and Ackerson, 1981; Zhao et al., 2005; Ding et al., 2005). While investigating this phenomenon would be outside the scope of the present research, the observation suggests that water-N interactions and confounding are topics pertinent not only for N management but also irrigation management. Just as water effects can cause misinterpretation of N sufficiency from optical canopy sensing, N effects can cause misinterpretation of water sufficiency from canopy temperature sensing. Additionally, while the use of the soil adjusted vegetation index (Huete, 1988) to estimate ET crop coefficients is a well-established practice (Bausch, 1993; Choudhury et al., 1994; Campos et al., 2017; Barker et al., 2018), N stress might alter the relationship between these two variables. As highlighted by Rudnick and Irmak (2014), future studies could develop methods of accounting for N effects on crop ET—perhaps involving optical canopy sensing.

4. Conclusion

This research highlighted the complexity of water effects on optical canopy sensing for late-season N management of corn. Water effects were found not to be always negligible on the Datt (1999) index and not to be always monotonic with water sufficiency. Water effects were also found to be influenced by genetics and/or previous crop and by interannual and intraseasonal weather differences. Unless in-season precipitation is negligible, water excess and water stress are likely to be temporary states which crops enter and exit for parts of the growing season, and the timing and severity of each round of water excess and water stress are likely to differ. Therefore, genotype, environment, and management jointly determine the canopy damage during water excess/ stress and the canopy recovery after water excess/ stress, ultimately affecting the magnitude and direction of water effects on optical canopy sensor data.

In light of this complexity, considerations of water-N interactions and confounding should be increasingly incorporated into precision agriculture. This research may be the first to develop an explicit method of accounting for water effects in optical canopy sensing for late-season N management

of corn. This new method has the potential to benefit four audiences: (1) rainfed growers who have minimal ability to alter water sufficiency, (2) irrigated growers who achieve low irrigation uniformity, (3) irrigated growers who do not use variable rate irrigation to compensate for natural heterogeneity in water sufficiency, and (4) irrigated growers who intentionally induce water stress on parts of the field because the irrigation water supply is inadequate for fully irrigating the entire field. More integrated thinking and more purposeful research will continue to be necessary for tackling all the challenges that water-N interactions and confounding can introduce to the management of both irrigation and N fertilizer.

Acknowledgments — The authors are grateful to Turner Dorr and Jacob Nickel for their involvement with data collection; to Gary Mahnken and Merle Still for their supporting roles in field management; to AirScout for their donation of aerial imagery products and services; and to Lindsay Corporation, Holzfasters Irrigation, Agri-Inject, SureFire Ag Systems, and Holland Scientific for their timely technical support. This research is based upon work that was jointly supported by the United States Department of Agriculture's National Institute of Food and Agriculture under award number 2016-68007-25066, "Sustaining agriculture through adaptive management to preserve the Ogallala aquifer under a changing climate", and under Hatch project #1015698; the Nebraska Corn Board under award number 88-R-1617-06; the Daugherty Water for Food Global Institute; and University of Nebraska-Lincoln Institute of Agriculture and Natural Resources.

References

- Bai, G., Ge, Y., Hussain, W., Baenzinger, P.S., Graef, G.L., 2016. A multi-sensor system for high throughput field phenotyping in soybean and wheat breeding. *Comput. Electron. Agric.* 128, 181–192. <https://doi.org/10.1016/j.compag.2016.08.021>
- Barker, J.B., Franz, T.E., Heeren, D.M., Neale, C.M.U., Luck, J.D., 2017. Soil water content monitoring for irrigation management: a geostatistical analysis. *Agric. Water Manag.* 188, 36–49. <https://doi.org/10.1016/j.agwat.2017.03.024>
- Barker, J.B., Neale, C.M.U., Heeren, D.M., Suyker, A.E., 2018. Evaluation of a hybrid reflectance-based crop coefficient and energy balance evapotranspiration model for irrigation management. *Trans. ASABE* 61 (2), 533–548. <https://doi.org/10.13031/trans.12311>
- Barnes, E.M., Clarke, T.R., Richards, S.E., Colaizzi, P.D., Haberland, J.A., Kostrzewski, M., Waller, P.M., Choi, C., Riley, E., Thompson, T.L., Lascano, R.J., Li, H., Moran, M.S., 2000. Coincident detection of crop water stress, nitrogen status and canopy density using ground-based multispectral data. In: Robert, P.C., Rust, R.H., Larson, W.E. (Eds.), *Proceedings of the Fifth International Conference on Precision Agriculture*. ASA-CSSA-SSSA, Madison, WI.

- Bausch, W.C., 1993. Soil background effects on reflectance-based crop coefficients for corn. *Remote Sens. Environ.* 46 (2), 213–222. [https://doi.org/10.1016/0034-4257\(93\)90096-G](https://doi.org/10.1016/0034-4257(93)90096-G)
- Blackmer, T.M., Schepers, J.S., 1995. Use of a chlorophyll meter to monitor nitrogen status and schedule fertigation for corn. *J. Prod. Agric.* 8 (1), 56–60. <https://doi.org/10.2134/jpa1995.0056>
- Blackmer, T.M., Schepers, J.S., 1996. Aerial photography to detect nitrogen stress in corn. *J. Plant Physiol.* 148 (3–4), 440–444. [https://doi.org/10.1016/S0176-1617\(96\)80277-X](https://doi.org/10.1016/S0176-1617(96)80277-X)
- Bronson, K.F., White, J.W., Conley, M.M., Hunsaker, D.J., Thorp, K.R., French, A.N., Mackey, B.E., Holland, K.H., 2017. Active optical sensors in irrigated durum wheat: nitrogen and water effects. *Agron. J.* 109 (3), 1060–1071. <https://doi.org/10.2134/agronj2016.07.0390>
- Campos, I., Neale, C.M.U., Suyker, A.E., Arkebauer, T.J., Gonçalves, I.Z., 2017. Reflectance-based crop coefficients REDUX: for operational evapotranspiration estimates in the age of high producing hybrid varieties. *Agric. Water Manag.* 187, 140–153. <https://doi.org/10.1016/j.agwat.2017.03.022>
- Choudhury, B.J., Ahmed, N.U., Idso, S.B., Reginato, R.J., Daughtry, C.S.T., 1994. Relations between evaporation coefficients and vegetation indices studies by model simulations. *Remote Sens. Environ.* 50 (1), 1–17. [https://doi.org/10.1016/0034-4257\(94\)90090-6](https://doi.org/10.1016/0034-4257(94)90090-6)
- Clay, D.E., Kim, K., Chang, J., Clay, S.A., Dalsted, K., 2006. Characterizing water and nitrogen stress in corn using remote sensing. *Agron. J.* 98 (3), 579–587. <https://doi.org/10.2134/agronj2005.0204>
- Datt, B., 1999. Visible/near infrared reflectance and chlorophyll content in eucalyptus leaves. *Int. J. Remote Sens.* 20 (14), 2741–2759. <https://doi.org/10.1080/014311699211778>
- Ding, L., Wang, K.J., Jiang, G.M., Biswas, D.K., Xu, H., Li, L.F., Li, Y.H., 2005. Effects of nitrogen deficiency on photosynthetic traits of maize hybrids released in different years. *Ann. Bot.* 96 (5), 925–930. <https://doi.org/10.1093/aob/mci244>
- El-Shikha, D.M., Barnes, E.M., Clarke, T.R., Hunsaker, D.J., Haberland, J.A., Pinter Jr., P.J., Waller, P.M., Thompson, T.L., 2008. Remote sensing of cotton nitrogen status using the canopy chlorophyll content index (CCCI). *Trans. ASABE* 51 (1), 73–82. <https://doi.org/10.13031/2013.24228>
- Fitzgerald, G.J., Rodriguez, D., Christensen, L.K., Belford, R., Sadras, V.O., Clarke, T.R., 2006. Spectral and thermal sensing for nitrogen and water status in rainfed and irrigated wheat environments. *Precis. Agric.* 7 (4), 233–248. <https://doi.org/10.1007/s11119-006-9011-z>
- Holland, K.H., Schepers, J.S., 2010. Derivation of a variable rate nitrogen application model for in-season fertilization of corn. *Agron. J.* 102 (5), 1415–1424. <https://doi.org/10.2134/agronj2010.0015>
- Holland, K.H., Schepers, J.S., 2013. Use of a virtual-reference concept to interpret active crop canopy sensor data. *Precis. Agric.* 14 (1), 71–85. <https://doi.org/10.1007/s11119-012-9301-6>
- Holland Scientific, 2018. Crop Circle ACS-430 Active Crop Canopy Sensor. Retrieved from. <https://hollandscientific.com/portfolio/crop-circle-acs-430/>

- Huete, A.R., 1988. A soil-adjusted vegetation index (SAVI). *Remote Sens. Environ.* 25 (3), 295–309. [https://doi.org/10.1016/0034-4257\(88\)90106-X](https://doi.org/10.1016/0034-4257(88)90106-X)
- Idso, S.B., Jackson, R.D., Pinter Jr., P.J., Reginato, R.J., Hatfield, J.L., 1981. Normalizing the stress-degree-day parameter for environmental variability. *Agric. Meteorol.* 24, 45–55. [https://doi.org/10.1016/0002-1571\(81\)90032-7](https://doi.org/10.1016/0002-1571(81)90032-7)
- Jackson, R.D., Idso, S.B., Reginato, R.J., Pinter Jr., P.J., 1981. Canopy temperature as a crop water stress indicator. *Water Resour. Res.* 17 (4), 1133–1138. <https://doi.org/10.1029/WR017i004p01133>
- Kendall, M.G., 1938. A new measure of rank correlation. *Biometrika* 30 (1–2), 81–93. <https://doi.org/10.1093/biomet/30.1-2.81>
- METER Group, 2018. SRS Spectral Reflectance Sensor: Operator's Manual. Retrieved from. http://manuals.decagon.com/Manuals/14597_SRS_Web.pdf
- Mon, J., Bronson, K.F., Hunsaker, D.J., Thorp, K.R., White, J.W., French, A.N., 2016. Interactive effects of nitrogen fertilization and irrigation on grain yield, canopy temperature, and nitrogen use efficiency in overhead sprinkler-irrigated durum wheat. *Field Crops Res.* 191, 54–65. <https://doi.org/10.1016/j.fcr.2016.02.011>
- Moran, M.S., Clarke, T.R., Inoue, Y., Vidal, A., 1994. Estimating crop water deficit using the relation between surface-air temperature and spectral vegetation index. *Remote Sens. Environ.* 49 (3), 246–263. [https://doi.org/10.1016/0034-4257\(94\)90020-5](https://doi.org/10.1016/0034-4257(94)90020-5)
- Radin, J.W., Ackerson, R.C., 1981. Water relations of cotton plants under nitrogen deficiency: III. Stomatal conductance, photosynthesis, and abscisic acid accumulation during drought. *Plant Physiol.* 67, 115–119. <https://doi.org/10.1104/pp.67.1.115>
- Rudnick, D.R., Irmak, S., 2014. Impact of nitrogen fertilizer on maize evapotranspiration crop coefficients under fully irrigated, limited irrigation, and Rainfed settings. *J. Irrig. Drain. Eng.* 140 (12), 04014039. [https://doi.org/10.1061/\(ASCE\)IR.1943-4774.0000778](https://doi.org/10.1061/(ASCE)IR.1943-4774.0000778)
- Rudnick, D.R., Irmak, S., Ferguson, R.B., Shaver, T.M., Djaman, K., Slater, G.P., Bereuter, A.M., Ward, N.C., Francis, D.D., Schmer, M.R., Wienhold, B.J., Van Donk, S.J., 2016. Economic return versus crop water productivity of maize for various nitrogen rates under full irrigation, limited irrigation, and Rainfed settings in south central Nebraska. *J. Irrig. Drain. Eng.* 142 (6), 04016017. [https://doi.org/10.1061/\(ASCE\)IR.1943-4774.0001023](https://doi.org/10.1061/(ASCE)IR.1943-4774.0001023)
- Scharf, P.C., Lory, J.A., 2002. Calibrating corn color from aerial photographs to predict sidedress nitrogen need. *Agron. J.* 94 (3), 397–404. <https://doi.org/10.2134/agronj2002.3970>
- Schepers, J.S., Blackmer, T.M., Wilhelm, W.W., Resende, M., 1996. Transmittance and reflectance measurements of corn leaves from plants with different nitrogen and water supply. *J. Plant Physiol.* 148 (5), 523–529. [https://doi.org/10.1016/S0176-1617\(96\)80071-X](https://doi.org/10.1016/S0176-1617(96)80071-X)
- Schlemmer, M.R., Francis, D.D., Shanahan, J.F., Schepers, J.S., 2005. Remotely measuring chlorophyll content in corn leaves with differing nitrogen levels and relative water content. *Agron. J.* 97 (1), 106–112. <https://doi.org/10.2134/agronj2005.0106>

- Shapiro, C.A., Wortmann, C.S., Walters, D.T., 2008. Fertilizer Suggestions for Corn. Extension Circular EC117. Retrieved from. University of Nebraska–Lincoln Extension, Lincoln, NE. <http://extensionpublications.unl.edu/assets/pdf/ec117.pdf>
- Shaver, T.M., Kruger, G.R., Rudnick, D.R., 2017. Crop canopy sensor orientation for late season nitrogen determination in corn. *J. Plant Nutr.* 40 (15), 2217–2223. <https://doi.org/10.1080/01904167.2017.1346681>
- Shiratsuchi, L.S., Ferguson, R.B., Shanahan, J.F., Adamchuk, V.I., Rundquist, D.C., Marx, D.B., Slater, G.P., 2011. Water and nitrogen effects on active canopy sensor vegetation indices. *Agron. J.* 103 (6), 1815–1826. <https://doi.org/10.2134/agronj2011.0199>
- Solari, F., Shanahan, J.F., Ferguson, R.B., Schepers, J.S., Gitelson, A.A., 2008. Active sensor reflectance measurements of corn nitrogen status and yield potential. *Agron. J.* 100 (3), 571–579. <https://doi.org/10.2134/agronj2007.0244>
- Tiling, A.K., O’Leary, G.J., Ferwerda, J.G., Jones, S.D., Fitzgerald, G.J., Rodriguez, D., Belford, R., 2007. Remote sensing of nitrogen and water stress in wheat. *Field Crops Res.* 104 (1–3), 77–85. <https://doi.org/10.1016/j.fcr.2007.03.023>
- Vachaud, G., Passerat de Silans, A., Balabanis, P., Vauclin, M., 1985. Temporal stability of spatially measured soil water probability density function. *Soil Sci. Soc. Am. J.* 49 (4), 822–828. <https://doi.org/10.2136/sssaj1985.03615995004900040006x>
- Ward, N.C., 2015. Nitrogen and Water Effects on Canopy Sensor Measurements for Site- Specific Management of Crops (Doctoral dissertation). Online at University of Nebraska–Lincoln, Lincoln, NE. <http://digitalcommons.unl.edu/agronhortdiss/91>
- Zhao, D., Reddy, K.R., Kakani, V.G., Reddy, V.R., 2005. Nitrogen deficiency effects on plant growth, leaf photosynthesis, and hyperspectral reflectance properties of sorghum. *Eur. J. Agron.* 22 (4), 391–403. <https://doi.org/10.1016/j.eja.2004.06.005>